Developmental Cell, Vol. 7, 491–501, October, 2004, Copyright ©2004 by Cell Press

Apoptotic Cells Can Induce Compensatory Cell Proliferation through the JNK and the Wingless Signaling Pathways

Hyung Don Ryoo, Travis Gorenc, and Hermann Steller*
Howard Hughes Medical Institute
The Rockefeller University
1230 York Avenue, Box 252
New York, New York 10021

Summary

In many metazoans, damaged and potentially dangerous cells are rapidly eliminated by apoptosis. In *Drosophila*, this is often compensated for by extraproliferation of neighboring cells, which allows the organism to tolerate considerable cell death without compromising development and body size. Despite its importance, the mechanistic basis of such compensatory proliferation remains poorly understood. Here, we show that apoptotic cells express the secretory factors *wingless (wg)* and *decapentaplegic (dpp).* When cells undergoing apoptosis were kept alive with the caspase inhibitor p35, excessive nonautonomous cell proliferation was observed. Significantly, *wg* signaling is necessary and, at least in some cells, also sufficient for mitogenesis under these conditions. Finally, we provide evidence that the DIAP1 antagonists *reaper* and *hid* can activate the JNK pathway and that this pathway is required for inducing *wg* and cell proliferation. These findings support a model where apoptotic cells activate signaling cascades for compensatory proliferation.

Introduction

Most metazoan cells have the ability to self-destruct when their death benefits the survival of the organism. Examples of such programmed cell death (PCD) include the elimination of damaged or supernumerary cells and the sculpting of body structures during embryo development (Jacobson et al., 1997; Hengartner, 2000). Apoptosis is a prominent and morphologically distinct form of PCD characterized by cellular condensation, caspase activation, and rapid engulfment of corpses by macrophages (Kerr et al., 1972; Yuan et al., 1993).

In the past two decades, significant progress has been made in understanding how cells initiate and execute apoptosis (Hengartner, 2000; Daniel and Korsmeyer, 2004; Salvesen and Abrams, 2004). At the multicellular level, however, relatively little is known about how apoptotic cells interact with neighboring cells in an epithelial layer. Studies in *Drosophila* indicate a robust communication mechanism between apoptotic cells and their living neighbors. For example, triggering massive cell death by X-ray irradiation or through genetic manipulation induces extracell proliferation (Haynie and Bryant, 1977; Milan et al., 1997). Such compensatory mechanisms may be essential to allow for the elimination of as many damaged or dangerous cells as needed without compromising organismal fitness. In spite of its importance, the underlying mechanisms are poorly understood.

Apoptosis in *Drosophila*, as in other animals, is executed by active caspases (Song et al., 1997; Fraser et al., 1997; Meier et al., 2000). A crucial inhibitor of caspases is DIAP1, which is required for the survival of all somatic cells of *Drosophila* embryos (Wang et al., 1999; Goyal et al., 2000; Lisi et al., 2000). In living cells, DIAP1 binds to caspases and inhibits their activity or ubiquitylates them for degradation (Wang et al., 1999; Wilson et al., 2002). Most, if not all, cells doomed to die express *reaper*, *hid*, and *grim*, which inhibit the antiapoptotic activity of DIAP1 (White et al., 1994; Grether et al., 1995; Chen et al., 1996). Once DIAP1 is bound to its antagonists, it undergoes autoubiquitylation for proteasomal degradation (Ryoo et al., 2002; Yoo et al., 2002), liberating caspases for the execution of apoptosis.

In this study, we show that cells stimulated to undergo apoptosis express mitogens, and when kept alive, exhibit strong growth-stimulating activity (see also Huh et al., 2004). Inhibition of DIAP1 is required for mitogen expression and stimulation of growth. Furthermore, we demonstrate that the Jun N-terminal kinase (JNK) pathway is activated in apoptotic cells. JNK signaling is required for *wg* induction and growth stimulation in this paradigm. Additionally, we provide evidence that the *wg* signaling pathway is required for compensatory proliferation. We propose that mitogenic signals from apoptotic cells may contribute to the maintenance of tissue homeostasis in healthy tissues and tumor growth in pathological conditions.

Results

diap1 Is Required for the Survival of Imaginal Disc Cells

Drosophila larval imaginal discs show a robust coordination of cell death and proliferation (Neufeld et al., 1998). Imaginal discs are subdivided into anterior (A) and posterior (P) compartments, within which cells have separate lineage and do not mix during development (Garcia-Bellido et al., 1973). *diap1* is essential for the survival of virtually all embryonic cells (Wang et al., 1999; Goyal et al., 2000; Lisi et al., 2000). Likewise, survival of imaginal disc cells depends on *diap1*. We generated $diap1^{22\text{-}8s/22\text{-}8s}$ cells through mitotic recombination (see Experimental Procedures). The $diap1^{22\text{-}8s}$ allele has an impaired ubiquitin-ligase activity and behaves as a hypomorphic loss-of-function allele in imaginal discs (Wilson et al., 2002; Ryoo et al., 2002). 18 hr after clonal induction, large numbers of $diap1^{22\text{-}8s/22\text{-}8s}$ cells were observed that labeled with anti-active caspase-3 antibody, which detects activated *Drosophila* effector caspases, drICE and DCP-1 (Figures 1B and 1C; Yu et al., 2002). After 72 hr of clonal induction, no $diap1^{22\text{-}8s/22\text{-}8s}$ cells were detected, whereas the +/+ twin spots had grown to sizable mosaic clones (Figure 1F). This indicates that

*Correspondence: steller@rockefeller.edu

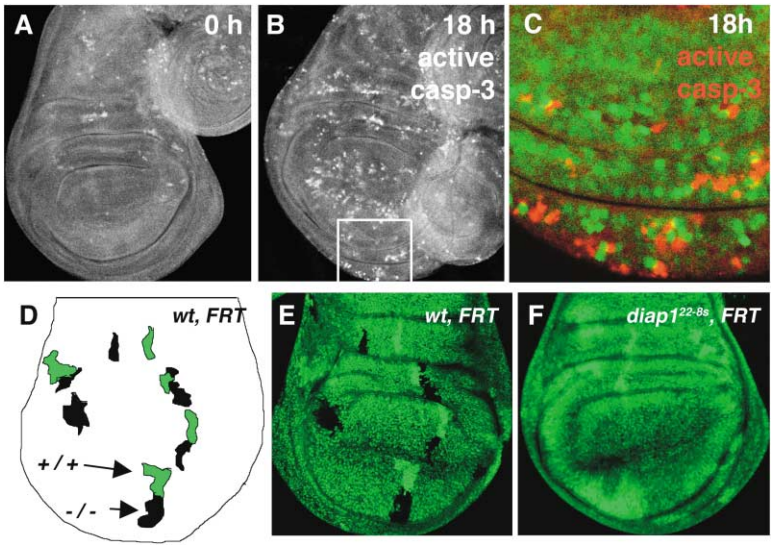

Figure 1. *diap1*$^{22\text{-}8s/22\text{-}8s}$ Cells Fail to Survive in Imaginal Discs

(A–C and F) Genotype: *hs-flp; diap1*$^{22\text{-}8s}$*, FRT80/hs-GFP, FRT80*. (A and B) Anti-active caspase-3 antibody labeling (white) in wing imaginal discs. (A) Before the induction of *diap1*$^{22\text{-}8s/22\text{-}8s}$ cells. (B and C) 18 hr after inducing *diap1*$^{22\text{-}8s/22\text{-}8s}$ clones through mitotic recombination. (B) Active caspase-3 single channel. The inset magnified in (C) shows anti-active caspase-3 antibody labeling (red) in many of the *diap1*$^{22\text{-}8s/22\text{-}8s}$ population, marked by the absence of GFP (green).

(D–F) *diap1*$^{22\text{-}8s/22\text{-}8s}$ cells are completely eliminated 3 days after mitotic recombination. (D and E) A wing disc with mosaic clones of a control chromosome. Genotype: *hs-flp; FRT80/hs-GFP, FRT80*. (D) is a schematic diagram of (E) showing that both control −/− clones (black) and +/+ sister clones (bright green) survive and proliferate. (F) *diap1*$^{22\text{-}8s/22\text{-}8s}$ cells do not survive, as evidenced by the lack of non-GFP population.

diap1$^{22\text{-}8s/22\text{-}8s}$ cells activate caspases and undergo apoptosis. Similar observations were made with *diap1*^{th5} (data not shown), a null allele with a premature stop codon. Despite widespread cell death, these animals developed into adults indistinguishable from that of wild-type, indicating that apoptosis in proliferating tissues can be effectively compensated, as previously reported (Haynie and Bryant, 1977; Milan et al., 1997).

diap1$^{22\text{-}8s/22\text{-}8s}$ Undead Cells Promote Imaginal Disc Growth

To understand how cell death is compensated for by cell proliferation, we considered two models (Figure 2A). In the "active model," dying cells secrete mitogens to induce proliferation of cells in the vicinity. By contrast, in the "passive model," the dying cells do not invoke mitogenic signaling. In this case, the absence of cells stimulates extraproliferation, for example, through physical changes in cell-cell boundaries or other indirect mechanisms. To test whether the active model plays a role in compensatory proliferation, apoptosis was initiated through upstream regulators, and then the execution was blocked by inhibiting caspases. The two different models make vastly different predictions about the consequence of keeping stressed cells alive. According to the passive model, the persistence of these "undead cells" should not stimulate any extra proliferation. By contrast, the active model predicts that prolonging the life of stressed cells by blocking the execution of apoptosis might lead to secretion of mitogens over a much longer period of time and hence cause the overgrowth of surrounding tissue.

We generated *diap1*$^{22\text{-}8/22\text{-}8s}$ cells in the P compartment, which subsequently led to their death during development. Despite the elimination of the *diap1*$^{22\text{-}8s/22\text{-}8s}$ population, the sister *diap1* +/+ population developed into a full-size P compartment (Figure 2C and Supplemental Figure S1A at http://www.developmentalcell.com/cgi/content/full/7/4/491/DC1/), confirming that cell death is compensated. Furthermore, these animals developed into adults indistinguishable from that of wild-type animals (data not shown).

To test if apoptotic cells play an active role in compensatory proliferation (Figure 2A), we blocked the execution of cell death in *diap1*$^{22\text{-}8s/22\text{-}8s}$ mosaic clones by overexpressing the baculovirus p35 caspase inhibitor (Clem et al., 1991). Expression of *p35* throughout the P compartment blocked the cell lethality of *diap1*$^{22\text{-}8s/22\text{-}8s}$ clones. These undead cells shifted toward the basal side of discs, but otherwise retained the ability to grow and proliferate to form sizable mosaic clones by the late 3rd instar stage (Figure 2D). Strikingly, these wing imaginal discs were significantly larger than control discs, averaging a 45% increase in size (Figure 2D and Supplemental Figure S1A), and the corresponding animals died during the pupal stage. A similar observation was made with another *diap1* allele, *diap1*$^{33\text{-}1s}$ (Supplemental Figures S1B and S1C). As previously reported, the expression of *p35* alone did not affect cell growth and proliferation (Neufeld et al., 1998). We also generated undead *diap1*$^{22\text{-}8s/22\text{-}8s}$ clones in the developing eye disc and observed tissue outgrowths (Figures 2E and 2F), indicating that this phenomenon is not tissue specific. Furthermore, these data suggest that active signaling plays a role in apoptosis-induced compensatory proliferation.

Undead Cells Induce Nonautonomous Cell Proliferation

In order to directly investigate the ability of undead cells to stimulate cell proliferation, we examined the pattern of BrdU incorporation in discs containing undead cells (Figure 3). Dronc is an apical caspase and a ubiquitylation target of DIAP1 (Wilson et al., 2002). We found that *diap1*$^{22\text{-}8s/22\text{-}8s}$ undead cells contain higher levels of Dronc (Supplemental Figure S2). As undead cells moved toward the basal side of imaginal discs, negative labeling of this population with GFP occasionally gave an inaccurate estimate of the clonal boundary. In addition, a few GFP-positive members of the wild-type population,

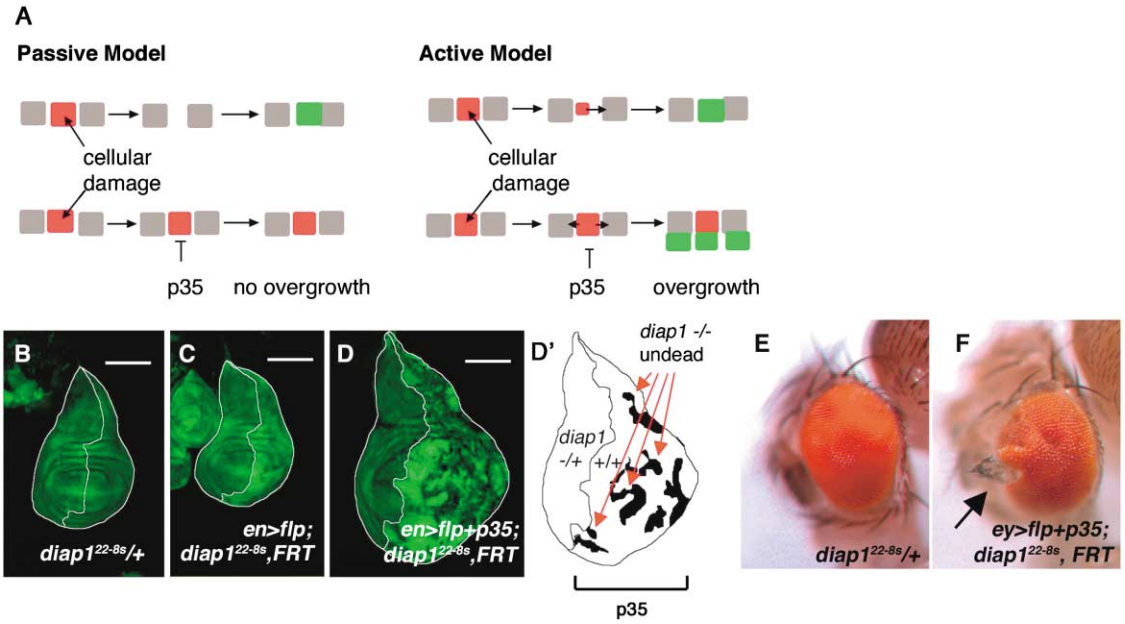

Figure 2. Active versus Passive Model of Cell Death and Compensatory Proliferation

(A) Two models of compensatory proliferation. Red cells indicate those where apoptosis has been initiated. Green cells are newborn cells. In the passive model, loss or absence of cells stimulates extraproliferation. In this model, blocking cell death execution also prevents compensatory proliferation. In contrast, the active model predicts that dying cells secrete mitogens as part of the cell death program. In this case, blocking the execution of apoptosis may result in an undead state, leading to persistent secretion of mitogens and tissue overgrowth.

(B–D) Experimental validation of the active model. *diap1*$^{+/+}$ and *diap1*$^{22\text{-}8s/+}$ are marked with GFP (green), and the *diap1*$^{22\text{-}8s/22\text{-}8s}$ cells are identified by the absence of GFP. The P compartment is on the right half of the disc and the A compartment is on the left half of the disc. The disc and compartment boundaries are outlined (white). Scale bars equal 100 μm.

(B) *diap1*$^{22\text{-}8s/+}$ wing disc as a control. Full genotype: *diap1*$^{22\text{-}8s}$*/ubi-GFP, FRT80*.

(C) A wing disc where mitotic recombination of *diap1*$^{22\text{-}8s}$ was induced within the P compartment. The A compartment consists exclusively of *diap1*$^{22\text{-}8s}$/+ cells (weak green), while the P compartment consists of mostly +/+ wild-type cells (bright green). Genotype: *en-Gal4/uas-flp; diap1*$^{22\text{-}8s}$*, FRT80/ubi-GFP, FRT80*.

(D) A wing imaginal disc where *diap1*$^{22\text{-}8s/22\text{-}8s}$ clones were generated and kept alive with *p35*. Genotype: *en-Gal4/uas-p35, uas-flp; diap1*$^{22\text{-}8s}$*, FRT80/ubi-GFP, FRT80*. These wing discs had significantly overgrown P compartments, supporting the active model.

(D′) A simplified schematic diagram of the wing disc shown in (D).

(E and F) Generating undead *diap1*$^{22\text{-}8s/22\text{-}8s}$ clones during eye development results in adults with eye outgrowth and fate transformation.

(E) A sibling control. Genotype: *uas-p35, uas-flp/CyO; diap1*$^{22\text{-}8s}$*, FRT80/ubi-GFP, FRT80*.

(F) An adult head with undead *diap1*$^{22\text{-}8s/22\text{-}8s}$ clones. Genotype: *ey-Gal4/uas-p35, uas-flp; diap1*$^{22\text{-}8s}$*, FRT80/ubi-GFP, FRT80*. Tissue outgrowth and fate transformation is indicated (arrow).

possibly macrophages, occasionally adhered to the *diap1*$^{22\text{-}8s/22\text{-}8s}$ population. Therefore, to unequivocally mark the *diap1*$^{22\text{-}8s/22\text{-}8s}$ cells, we used anti-Dronc antibody labeling as the clonal marker (Figures 3B and 3D). When undead *diap1*$^{22\text{-}8s/22\text{-}8s}$ clones were generated in the P compartment, we found significantly more BrdU-labeled cells, compared to the control A compartment (Figures 3A–3C). BrdU incorporation occurred much more frequently within the vicinity of *diap1*$^{22\text{-}8s/22\text{-}8s}$ cells (Figure 3D), suggestive of a diffusive mitogen emanating from undead cells. To use another experimental paradigm, we also expressed the DIAP1 antagonist Hid together with the caspase inhibitor *p35*. Cells expressing *hid* and *p35* can be marked with the anti-active caspase-3 antibody (Ryoo et al., 2002; Yoo et al., 2002), since p35 specifically blocks the activity of effector caspases, but not their activation (Yu et al., 2002). Under these conditions, undead cells were distributed throughout the entire P compartment (Figure 3E). Once again, increased BrdU incorporation was observed both within the P compartment and in the A compartment cells near the A/P boundary, suggesting that secretory mitogens are activated by *hid*-expressing cells (Figures 3D and 3E). These results show that blocking *diap1* function initiates a nonautonomous proliferation response.

Undead Cells Express Putative Mitogens

Next, we asked what mitogens may be induced by apoptotic cells. We focused our attention on secretory factors known to have mitogenic activities in *Drosophila,* including *wingless* (*wg*) and *decapentaplegic* (*dpp*). *wg* is a Wnt homolog that acts both as a morphogen and a mitogen (Neumann and Cohen, 1996; Zecca et al., 1996). In wild-type wing imaginal discs, *wg* is expressed in a specific pattern, including the dorso/ventral (D/V) boundary (Figure 4A). When *diap1*$^{22\text{-}8s/22\text{-}8s}$ cells were kept alive with *p35*, *wg* was induced within these undead cells (Figures 4B and 4C). *wg* induction was also found with a null allele of *diap1*, *th5* (Figure 4D). To test whether *wg* is induced autonomously, we used a *wg-lacZ* reporter with a nuclear localization sequence. The *diap1*$^{22\text{-}8s/22\text{-}8s}$ cells were marked positively for higher Dronc levels, as these undead cells shifted basally and

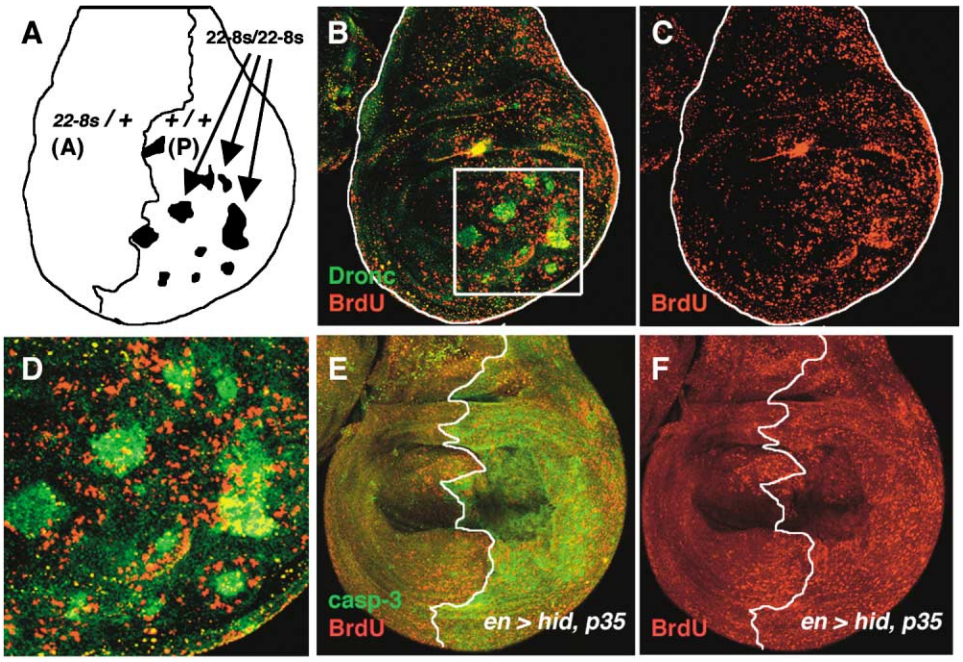

Figure 3. Undead Cells Promote Nonautonomous Proliferation

The A/P compartment boundary is outlined (white). BrdU incorporation is in (red).

(A–D) Apoptosis was initiated by generating *diap1*$^{22\text{-}8s/22\text{-}8s}$ clones and kept alive by expressing *p35*. Genotype: *en-Gal4/uas-p35, uas-flp; diap1*$^{22\text{-}8s}$*, FRT80/ubi-GFP, FRT80*.

(A) Schematic diagram of this wing disc.

(B) *diap1*$^{22\text{-}8s/22\text{-}8s}$ clones are marked by stronger anti-Dronc antibody immunoreactivity (green). BrdU incorpoation is also shown.

(C) BrdU-only channel shows enhanced cell proliferation in the P compartment.

(D) A magnified image of the inset in (B) (green).

(E and F) *hid* and *p35* were expressed in the P compartment to generate an alternate form of undead cells. Genotype: *uas-hid; uas-p35/en-Gal4*.

(E) Anti-active caspase-3 antibody labeling (green) marks the posterior compartment.

(F) BrdU-only channel.

negative marking by GFP gave inaccurate clonal boundaries for the *diap1*$^{22\text{-}8s/22\text{-}8s}$ population. Here, the nuclear lacZ expression was found strictly within the *diap1*$^{22\text{-}8s/22\text{-}8s}$ population (Supplemental Figure S3). To test whether overexpression of *hid* and *p35* activated *wg*, we generated mosaic clones expressing *hid* and *p35* for 72 hr. Again, the *hid*- and *p35*-expressing clones showed autonomous induction of *wg* (Figures 4E and 4F). These results demonstrate that eliminating *diap1* function leads to the induction of *wg* expression.

dpp is another secretory factor that acts as a morphogen, mitogen, and survival factor (Burke and Basler, 1996; Moreno et al., 2002; Martin-Castellanos and Edgar, 2002). In wing imaginal discs, *dpp* is normally expressed in the A compartment, alongside the A/P boundary (Figure 4G). Generation of *diap1*$^{22\text{-}8s/22\text{-}8s}$ undead cells led to the induction of *dpp-lacZ* (Figures 4H and 4I). Double labeling with anti-Dronc indicated that *dpp-lacZ* induction was autonomous in these cells (Supplemental Figure S3). Ectopic *dpp-lacZ* was also observed in imaginal discs harboring *diap1*$^{th5/th5}$ clones (Figure 4J). Moreover, cells overexpressing *hid* and *p35* within the P compartment induced *dpp-lacZ* expression (Figures 4K and 4L). These results demonstrate that cells stimulated to undergo apoptosis can activate the expression of *wg* and *dpp*.

The degree of *wg* and *dpp* induction in the undead cells varied depending on its relative position within a wing disc, with stronger induction observed in the wing pouch region. Although the cause for this variation is unclear, the degree of *wg* and *dpp* induction correlates with the sensitivity to activate apoptosis and JNK signaling. Therefore, we speculate that the degree of *wg* and *dpp* induction may be, in part, a result of a cell's sensitivity to activate the apoptotic program.

wg Signaling Is Required for Cell Proliferation

In order to test whether the *wg* pathway is required for compensatory cell proliferation, we conditionally abrogated the response to *wg* signaling. *wg* signaling is mediated by the transcription factor TCF, which can be inhibited by overexpression of the N-terminal deleted form of TCF (*TCF*^{DN}) (van de Weterling et al., 1997). We conditionally activated *TCF*^{DN} along with *hid* and *p35* in the wing disc throughout the P compartment. For this purpose, we used the Gal4/Gal80^{ts} system to temporally control transgene expression (McGuire et al., 2003). Under these conditions, Hid protein accumulated at higher levels closer to the A/P border (Figures 5B–5E), but lower levels of Hid in some parts of the P compartment were difficult to detect, due to the fixation protocol required for BrdU labeling. However, the *engrailed* promoter used in this study drives transgene expression in all cells of the P compartment, as verified by antibody labeling

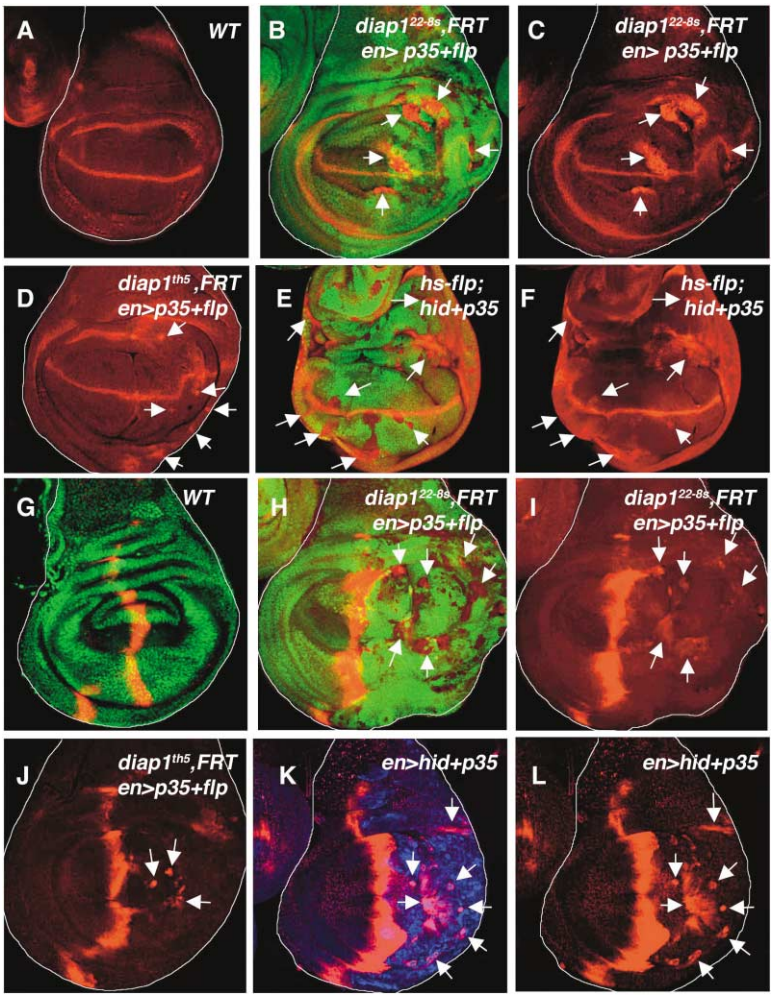

Figure 4. Undead Cells Activate *wg* and *dpp*

(A–C) *wg* is activated in *diap1*$^{22\text{-}8s/22\text{-}8s}$ cells kept alive with *p35*. *wg* expression is visualized by anti-WG antibody labeling (red).

(A) A wild-type wing imaginal disc.

(B and C) Ectopic *wg* expression is found in *diap1*$^{22\text{-}8s/22\text{-}8s}$ undead cells (arrows). Genotype: *en-Gal4/uas-p35, uas-flp; diap1*$^{22\text{-}8s}$*, FRT80/ubi-GFP, FRT80*. (B)The undead cells are marked by the absence of GFP (green).

(D) A wing disc containing *diap1*$^{th5/th5}$ clones kept alive with *p35*. Genotype: *en-Gal4, dpp-lacZ/uas-p35, uas-flp; diap1*^{th5}*, FRT80/ubi-GFP, FRT80*. Ectopic *wg* (arrows) is observed.

(E and F) Ectopic expression of *hid* and *p35* also activates ectopic *wg* expression (arrows). The ectopic expression clones are marked by the absence of GFP (green). Genotype: *uas-hid/hs-flp; uas-p35/tub>y+ GFP>Gal4*.

(F) WG single channel.

(G–I) *dpp-lacZ* is activated in *diap1*$^{22\text{-}8s/22\text{-}8s}$ undead cells as shown by anti-β-gal antibody labeling (red). Undead cells are marked by the absence of GFP (green).

(G) *dpp-lacZ* expression in wild-type imaginal discs.

(H and I) Ectopic *dpp-lacZ* expression is seen in *diap1*$^{22\text{-}8s/22\text{-}8s}$ undead cells (arrows). Genotype: *en-Gal4, dpp-lacZ/uas-p35, uas-flp; diap1*$^{22\text{-}8s}$*, FRT80/ubi-GFP, FRT80*.

(J) Ectopic *dpp-lacZ* is also observed in *diap1*$^{th5/th5}$ clones kept alive with *p35*. Genotype: *en-Gal4, dpp-lacZ/uas-p35, uas-flp; diap1*^{th5}*, FRT80/ubi-GFP, FRT80*.

(K and L) Ectopic expression of *hid* and *p35* activate ectopic *dpp-lacZ*. Anti-β-gal antibody labeling shows ectopic *dpp-lacZ* expression (arrows). Genotype: *uas-hid; uas-p35/en-Gal4*.

(K) Double labeling with anti-Hid antibody (blue) shows the P compartment.

under optimal conditions (e.g., see Figure 4K; Yoo et al., 2002). Interestingly, coexpression of *hid*, *p35*, and *TCF*^{DN} for 12 hr severely diminished BrdU incorporation (Figures 5B and 5C). A similar effect on BrdU incorporation was also observed when we induced *p35* and *TCF*^{DN} without *hid* (Figure 5F). After 24 hr, BrdU incorporation within the P compartment was almost completely suppressed in those parts of the wing discs with high transgene expression levels (Figures 5D and 5E). Under these conditions, the A compartment cells immediately neighboring the Hid-expressing cells appear to retain elevated BrdU incorporation; this is suggestive of a nonautonomous proliferative response (Figures 5D and 5E). Taken together, these experiments suggest that *wg* signaling is required for both the basal level of cell division in wing discs as well as the proliferation induced in response to apoptotic stimuli.

wg Signaling Can Stimulate Cell Proliferation

We also tested whether the activation of the *wg* signaling pathway is sufficient to promote cell proliferation in imaginal discs. For this purpose, we expressed a constitutively active Armadillo (Δ*arm*), a coactivator of TCF (Zecca et al., 1996; van de Weterling et al., 1997). Mosaic clones expressing Δ*arm* were generated and examined for BrdU incorporation and clonal growth. After 72 hr of clonal induction, Δ*arm*-expressing clones in the wing disc periphery gave larger clones compared to those of the control clones expressing *lacZ* (Figures 5G–5J). Moreover, Δ*arm*-expressing clones had enhanced BrdU incorporation compared to the control clones (Figures 5G–5J). These observations are consistent with the mitogenic role of *wg* in certain parts of the wing imaginal disc. However, activating *wg* signaling alone did not promote clonal growth in the distal parts of wing imaginal discs. This indicates that, at least in this region of the disc, activating *wg* alone is not sufficient to promote proliferation and suggests a requirement for other factors.

The JNK Pathway Is Required for the Induction of *wg* and Growth Stimulation

To investigate how the inhibition of *diap1* may lead to mitogen expression, we focused our attention on Dronc and the Jun N-terminal Kinase (JNK) pathway. Dronc has been recently implicated in compensatory proliferation (Huh et al., 2004), and its activity can be inhibited by the expression of *dronc*^{DN} (Meier et al., 2000). In addition, we considered the JNK signaling pathway as a candidate, since its activity is known to correlate with many

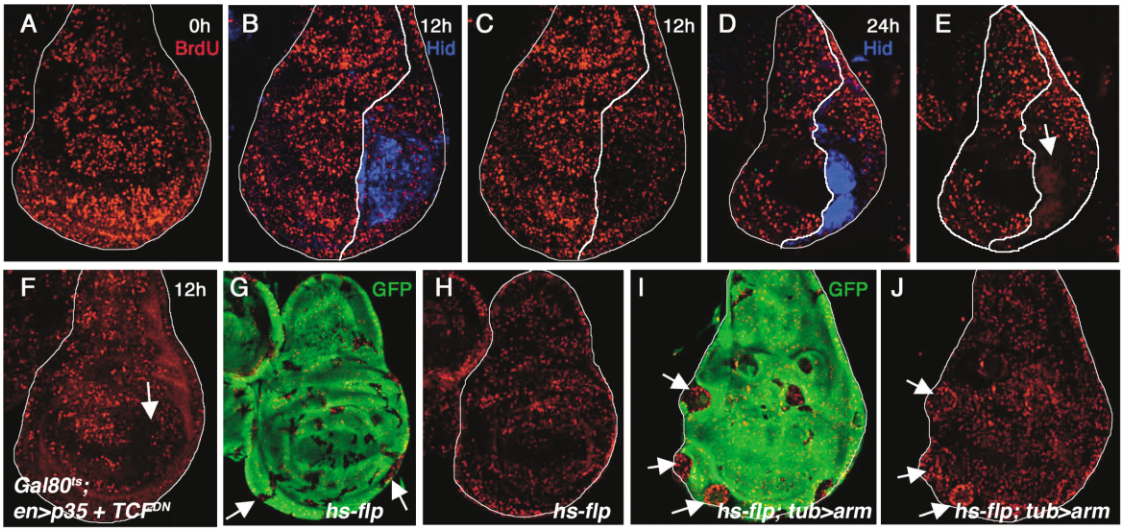

Figure 5. *wg* Signaling Is Required for Cell Proliferation

BrdU incorporation is shown (red) in all panels.

(A–E) Temporal induction of *hid*, *p35*, and TCF^{DN} suppresses cell proliferation. The A/P compartment boundary is outlined in white. Anti-Hid antibody labeling in blue. Hid accumulates at higher levels near the A/P boundary but the *en* promoter used here drives transgene expression throughout the P compartment (also see Figure 4K). Genotype: *uas-hid/+; uas-p35, uas-*TCF^{DN}*/en-Gal4; tub-*$Gal80^{ts}$.

(A) Uninduced control wing disc.

(B and C) BrdU incorporation is diminished after 12 hr of transgene induction.

(C) BrdU single channel of the image in (B).

(D and E) Inducing transgenes for 24 hr lead to an almost complete block in cell proliferation (arrow), correlating with the level of Hid protein (blue).

(F) Control disc without *uas-hid* shows that TCF^{DN} blocks cell cycle progression. Genotype: *uas-p35, uas-*TCF^{DN}*/en-Gal4; tub-*$Gal80^{ts}$.

(G–J) Activation of *wg* signaling promotes cell proliferation. Ectopic expression clones were generated 72 hr prior to dissection.

(G and H) Mosaic clones expressing *lacZ* as control. Genotype: *hs-flp; tub>GFP>Gal4/uas-lacZ*.

(G) GFP (green) and BrdU double labeling.

(H) BrdU single labeling.

(I and J) Mosaic clones expressing Δ*arm* was generated to activate the *wg* signaling pathway. Genotype: *hs-flp; tub>GFP>Gal4/uas-*Δ*arm*.

(I) GFP and BrdU double labeling.

(J) BrdU single channel. These discs have mosaic clones larger than those of control (G) and enhanced BrdU incorporation. Compare the clones indicated by arrows.

forms of stress-provoked apoptosis, including disruption of morphogens, cell competition, and *rpr* expression (Adachi-Yamada et al., 1999; Moreno et al., 2002; Kuranaga et al., 2002). In *Drosophila*, the JNK pathway can be effectively blocked by the expression of *puckered (puc)*, which encodes a phosphatase that negatively regulates JNK (Martin-Blanco et al., 1998).

To induce patches of undead cells, we generated wing imaginal discs with mosaic clones expressing *hid* and *p35*. 48 hr after induction, these imaginal discs contained *hid*-expressing clones that autonomously induced *wg* (see Figures 4E and 4F). Using this experimental setup, we tested whether additional expression of either $dronc^{DN}$ or *puc* blocks *wg* induction in undead cells. When $dronc^{DN}$ was coexpressed, a subset of the *hid*-expressing population was still able to induce *wg* (Figures 6A and 6B). In contrast, when *puc* was coexpressed, *wg* induction by *hid* was almost completely blocked (Figures 6C and 6D). These results provide evidence that the JNK pathway is required for *wg* induction under these conditions but fail to uncover a similar requirement for Dronc.

To independently investigate the role of *puc* and $dronc^{DN}$ in compensatory proliferation, we measured the size of wing discs harboring undead cells and compared them with those of the sibling controls (Figure 6I). Under our experimental conditions, wing discs harboring *hid*- and *p35*-expressing clones were on average 53% larger than their sibling controls ($p < 0.001$) (Figure 6I, columns 1 and 2). Coexpression of *puc* within these undead clones significantly limited growth, resulting in only a small increase in wing disc size that was not statistically significant (Figure 6I, columns 3 and 4). In contrast, coexpression of $dronc^{DN}$ did not limit growth (Figure 6I, columns 5 and 6). Wing size measurements also correlated with the degree of *wg* induction. The larger size of discs harboring *hid*- and *p35*-expressing cells is not due simply to extra cell survival. First, these undead cells are derived from the normal lineage. Second, the size of wing discs expressing *hid, p35*, and *puc* serves as a control (Figure 6I, columns 3 and 4). In this case, although a large number of undead cells were generated, no significant increase in disc size was observed, in stark contrast to the discs expressing *hid* and *p35* only. We conclude that the JNK pathway is required for the nonautonomous growth promoting activity of the undead cells.

Reduction of *puckered* Enhances *wg* Induction and Growth Stimulation

To confirm a role of *puc* in imaginal disc growth, we coexpressed *rpr* and *p35* in wild-type and $puc^{-/+}$ imaginal discs. Like *hid, rpr* is a DIAP1 antagonist, but with a weaker cell killing activity when overexpressed in

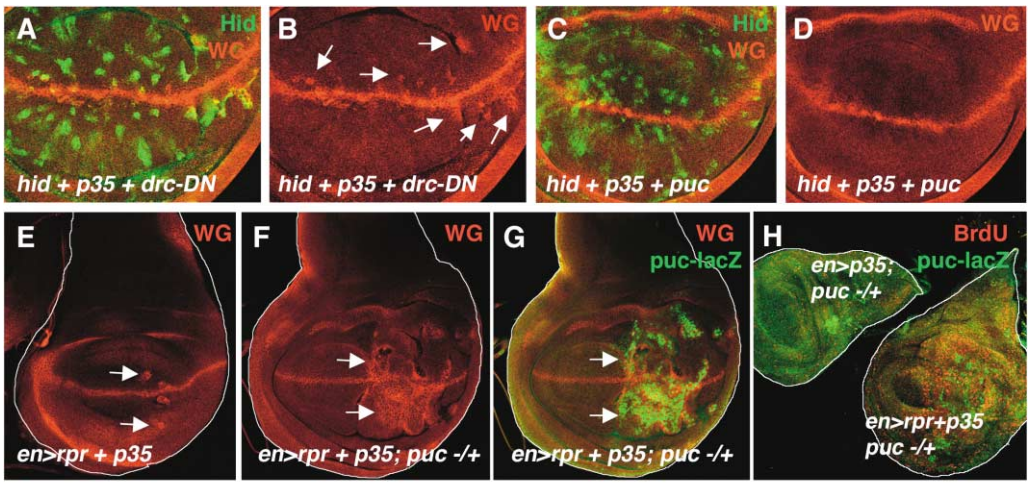

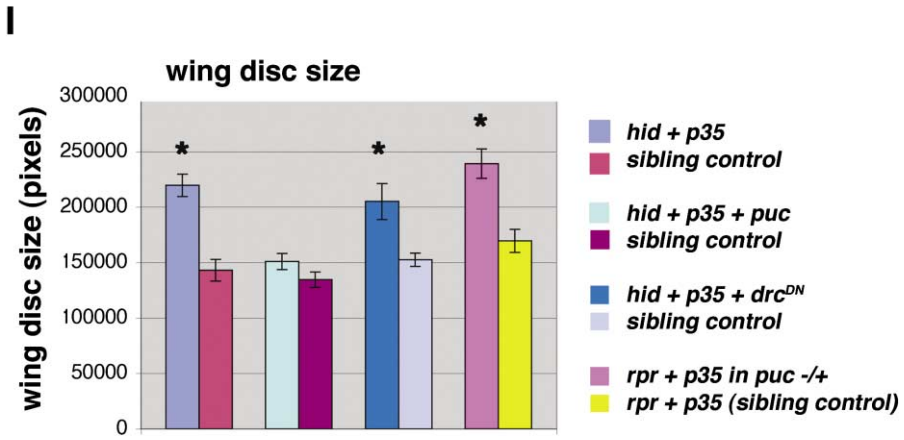

Figure 6. The JNK Pathway Is Required for *wg* Induction and Growth Stimulation

(A and B) Blocking the apical caspase, *dronc*, through dominant-negative *dronc* (*dronc*^{DN}) expression does not inhibit *wg* induction in undead cells. Genotype: *uas-hid/hs-flp; uas-p35/tub>GFP>Gal4 ; uas-dronc*^{DN}/+.

(A) Double labeling with anti-Hid (green) and anti-WG (red) antibodies.

(B) Anti-WG single channel shows *wg* induced within a subset of *hid*-expressing cells (arrows).

(C and D) Blocking the JNK pathway through *puckered (puc)* expression blocks *wg* induction in undead cells. Genotype: *uas-hid/hs-flp; uas-p35/tub>GFP>Gal4; uas-puc/+*.

(C) Double labeling with anti-Hid (green) and anti-WG (red) antibodies.

(D) Anti-WG single channel shows little, if any, induction of *wg* within the *hid*-expressing cells.

(E) *rpr* and *p35* were expressed within the P compartment and *wg* expression visualized by anti-WG antibody labeling (red). Genotype: *uas-rpr; uas-p35/en-Gal4*. Ectopic *wg* appears in a few patches (arrows).

(F and G) *rpr* and *p35* were expressed in *puc*^{E69}/+ background. Genotype: *uas-rpr; uas-p35/en-Gal4; puc*^{E69}/+.

(F) *wg* expression is strongly activated within the P compartment, compared to the control shown in (E).

(G) Double labeling with anti-β-gal antibody (green) shows that *puc-lacZ* expression correlates with ectopic *wg* expression (red). Since the reporter of *puc-lacZ* has a nuclear localization signal-tag, anti-β-gal antibody labeling detects the nuclei, whereas anti-WG antibody labels the cytoplasm.

(H) BrdU incorporation (red) and *puc-lacZ* expression (green) in wing imaginal discs. On the upper left is a control disc expressing *p35* in *puc*^{E69}/+ background. Genotype: *uas-p35/en-Gal4; puc*^{E69}/+. On the lower right is a disc coexpressing *rpr* and *p35* within the P compartment in *puc*^{E69}/+ background. Genotype: *uas-rpr/+; uas-p35/en-Gal4; puc*^{E69}/+. The latter disc shows significantly increased BrdU incorporation and larger disc size as compared to the controls. Notably, BrdU incorporation occurs nonautonomously from *puc-lacZ* expressing cells.

(I) Size measurement of wing discs containing undead cells. Columns 1–6 represent discs where undead mosaic clones were induced 48 hr prior to dissection (see Experimental Procedures). Genotype: *uas-hid/(hs-flp); uas-p35/tub>GFP>Gal4; uas-X*. The transgenes expressed are indicated on the right of the graph. The sibling controls lack *hs-flp*, but were otherwise raised in the same environment. Asterisks indicate those discs that give a statistically significant size difference compared to sibling controls. n is the number of samples analyzed. Columns 1 and 2: Wing discs containing *hid-, p35*-expressing clones were on average 54% larger than their sibling controls ($p < 0.001$; $n = 21$). Columns 3 and 4: When the JNK pathway was blocked in these clones through coexpression of *puc*, these wing discs were on average only 12% larger than their sibling controls, and not statistically significant ($n = 16$). Columns 5 and 6: When the *dronc*^{DN} was coexpressed in the mosaic clones, these wing discs were 35% larger than their sibling controls and comparable in size to those in column 1 ($p < 0.01$; $n = 15$). Columns 7 and 8: Genotype: *uas-rpr; uas-p35/en-Gal4; (puc)/+*. Discs expressing *rpr* and *p35* in the posterior compartment. *puc*$^{-/+}$ background enhanced the wing disc size on average 41%, compared to the sibling controls without the *puc* mutation ($p < 0.002$; $n = 26$).

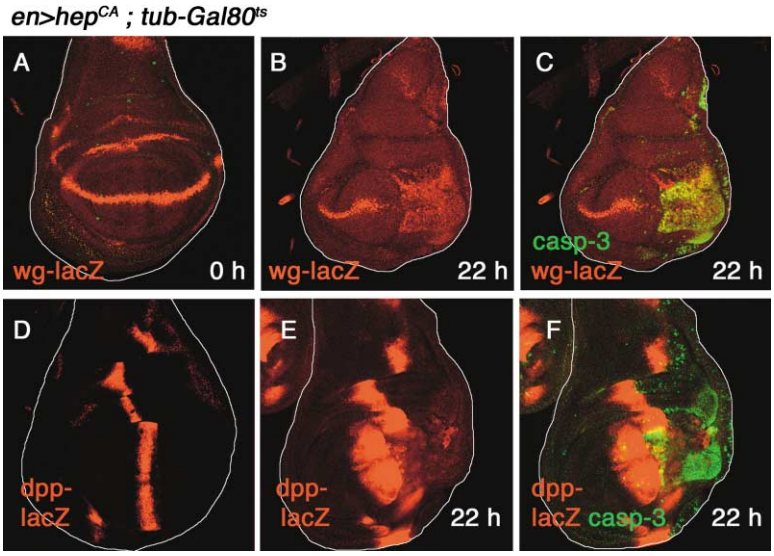

Figure 7. *hep*^{CA} Activates *wg-lacZ* and *dpp-lacZ* in Apoptotic Cells

Time course analysis of genes activated by *hep*^{CA}.

(A–C) *wg-lacZ* induction by *hep*^{CA}. Genotype: *wg-lacZ, en-Gal4/uas- hep*^{CA}*; tub-Gal80*^{ts}.

(A) Control wing disc kept in restrictive temperature shows a *wg-lacZ* pattern indistinguishable from wild-type.

(B and C) When *hep*^{CA} was induced for 22 hr at 29°C, *wg-lacZ* was induced as evidenced by anti-β-gal antibody labeling (red). These cells shifted basally, and as a result, the *wg-lacZ* pattern in the A compartment is partially out of focus.

(C) *wg-lacZ* expressing cells are apoptotic as evidenced by double labeling with anti-active caspase-3 antibody (green).

(D–F) *dpp-lacZ* is induced by *hep*^{CA}. Genotype: *dpp-lacZ, en-Gal4/+; uas-hep*^{CA}*/tub-Gal80*^{ts}.

(D) A control wing disc with a wild-type *dpp-lacZ* expression pattern.

(E and F) When *hep*^{CA} was induced for 22 hr within the P compartment, *dpp-lacZ* was induced as evidenced by anti-β-gal antibody labeling (red). (F) Double labeling with anti-caspase-3 antibody shows that many *dpp-lacZ*-expressing cells are apoptotic.

imaginal disc cells (e.g., Goyal et al., 2000; Lisi et al., 2000). In a *puc*$^{+/+}$ background, a small amount of ectopic *wg* expression was observed, indicative of *rpr*'s weaker DIAP1 inhibiting activity (Figure 6E). In contrast, ectopic *wg* expression was strongly enhanced in *puc*$^{-/+}$ discs (Figures 6E–6G). Because the *puc* allele used, *puc*^{E69}, also acts as a *lacZ* reporter, JNK pathway induction could be monitored simultaneously (Martin-Blanco et al., 1998). *wg* induction in undead cells correlated very well with *puc-lacZ* expression, with a stronger induction at the center of the wing pouch (Figure 6G). These results further support the role of JNK in the induction of *wg*.

We next tested whether the reduction of *puc* had an effect on apoptosis-induced cell proliferation. Whereas *puc*$^{-/+}$ discs expressing only *p35* had BrdU incorporation similar to wild-type discs, coexpression of *rpr* and *p35* in *puc*$^{-/+}$ led to a significant increase in BrdU incorporation (Figure 7H). Also, the size of these discs were on average 41% larger than those coexpressing *rpr* and *p35* in a *puc*$^{+/+}$ background (Figure 6I). Taken together, these results show that *diap1* inhibition leads to JNK activation and that JNK activity promotes *wg* induction and cell proliferation.

Active JNK Signaling Induces *wg-lacZ* and *dpp-lacZ* Expression in Apoptotic Cells

To directly test if JNK signaling can activate *wg* and *dpp* expression, we conditionally expressed *hep*^{CA}, a constitutively active form of *hemipterous* (*hep*), the *Drosophila* JNK kinase (Adachi-Yamada et al., 1999). Expression of *hep*^{CA} caused induction of *wg-lacZ* within 22 hr (Figures 7A–7C) and to a lesser extent also *dpp-lacZ* (Figures 7D–7F). These β-gal-expressing cells shifted basally and were apoptotic as assayed by anti-active caspase-3 antibody labeling. Hid protein levels were also elevated in these cells (Supplemental Figure S4). Significantly, since we did not use *p35* to block apoptosis in this experiment, this demonstrates that *wg* and *dpp* can be induced not only in undead cells, but also in "real" apoptotic cells.

Discussion

In many animal tissues, injury-provoked cell death is compensated for by extracell proliferation of neighboring cells. In *Drosophila*, apoptosis in response to cellular injury, such as irradiation, is typically mediated by the IAP antagonists *rpr*, *hid*, and *grim* (White et al., 1994; Grether et al., 1995, Chen et al., 1996; Brodsky et al., 2000, Zhou and Steller, 2003). Here, we provide evidence that these central apoptotic regulators can also control the activity of mitogenic pathways. In particular, inhibition of DIAP1, either via expression of Reaper and Hid or by mutational inactivation, led to the induction of the putative mitogens *wg* and *dpp*. When apoptosis was initiated through DIAP1 inhibition but cells were kept alive by blocking caspases, the resulting "undead cells" exhibited strong mitogenic activity and stimulated tissue overgrowth. Inhibiting *wg* signaling with a conditional *TCF*^{DN} blocked cell proliferation in imaginal discs, indicating that *wg* has an essential mitogenic function. Finally, we provide evidence that the JNK pathway mediates mitogen expression and imaginal disc overgrowth in response to *rpr* and *hid*. Based on these results, we propose that apoptotic cells actively signal to induce compensatory proliferation (Figure 8). DIAP1 inhibits both caspases (Wang et al., 1999; Wilson et al., 2002) as well as dTRAF1 (Kuranaga et al., 2002). According to this model, when DIAP1 is inhibited in response to cellular injury, the JNK pathway is activated and *wg/dpp* are induced in apoptotic cells. Secretion of these factors stimulates growth of proliferation-competent neighboring cells and leads to compensatory proliferation.

Recently, Hay and colleagues independently reported that the proapoptotic genes *hid* and *dronc* can activate cell proliferation (Huh et al., 2004). However, their model differs from ours in several important ways. Based on negative results from RNAi experiments, Huh et al. concluded that *diap1* is not involved in compensatory proliferation and proposed that Dronc is activated by an

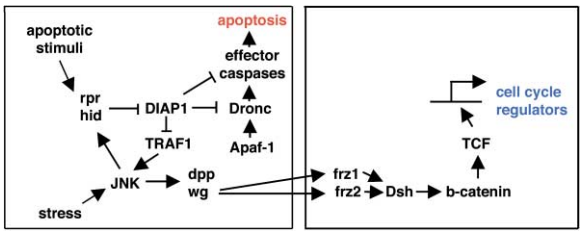

Figure 8. Model for Apoptosis-Induced Compensatory Proliferation

Various cellular damage and stress converge on the expression of *rpr*, *hid*, and *grim* in *Drosophila*. In addition to activating caspases for cell death execution, inhibition of DIAP1 results in the activation of the JNK pathway and *dpp*, *wg* expression. Expression of *wg* leads to the activation of a signal transduction cascade that involves the receptors frz1 and frz2 and the transcription factor TCF. This activates cell cycle progression in adjacent, proliferation-competent cells, presumably through the transcriptional regulation of cell cycle regulators.

unconventional mechanism that bypasses *diap1*. In contrast, we provide clear genetic evidence that *diap1* is involved in compensatory proliferation. Overall, similar results were obtained with hypomorphic *diap1* alleles (*diap1*$^{22\text{-}8s}$, *diap1*$^{33\text{-}1s}$), a null allele (*diap1*^{th5}), and inactivation of *diap1* by expression of Reaper and Hid. However, whereas expression of p35 effectively blocked apoptosis of *diap1*$^{22\text{-}8s/22\text{-}8s}$ cells and in response to Reaper/Hid, it only partially suppressed the death of *diap1*$^{th5/th5}$ cells. Consequently, the generation of undead cells was less efficient with the *diap1*^{th5} mutation. Moreover, our results suggest that the JNK pathway transduces the signal to activate mitogen expression and cell proliferation. As IAPs have been shown to ubiquitylate TRAFs in both mammals and *Drosophila* (Kuranaga et al., 2002; Li et al., 2002) and since we did not find evidence for Dronc in growth promotion, it is attractive to speculate that JNK is regulated through direct DIAP1/TRAF1 interaction (Figure 8).

Many of our results were obtained with undead cells, i.e., cells stimulated to undergo apoptosis but rescued from death by caspase inhibition. Consequently, it may be argued that mitogenic signaling under these conditions is a unique property of undead cells and not physiologically relevant. However, we show that JNK activation induces expression of *wg* and *dpp* autonomously in "genuine" apoptotic cells (Figure 7). Therefore, we favor the view that extending the life of doomed cells by p35 expression simply enhances a phenomenon that is otherwise transient and difficult to observe. Rapid clearance of apoptotic cells is presumably important to limit their mitogenic activity to achieve compensatory growth, as opposed to the tissue overgrowths seen with undead cells. It has been reported that *wg*, *dpp*, and *hh* are involved in the regeneration of fragmented imaginal discs, a phenomenon in which cut and cultured imaginal disc fragments undergo massive proliferation (Bryant, 1971; Gibson and Schubiger, 1999). In this paradigm, mitogen expression persists at the wound sites, resulting in cell fate respecification as well as proliferation. This aspect of persistent mitogen expression is similar to the situation in undead cells. However, apoptotic cells seldom interfere with cell fate, likely because they do not persist long enough to secrete levels of mitogens that are sufficient to alter cell fate decisions. On the other hand, it is conceivable that cells with impaired apoptosis, such as cancer cells, may have excessive and undesirable mitogenic and morphogenetic activity (see below).

The JNK Pathway Mediates Compensatory Proliferation

Another important unresolved question is why compensatory proliferation is seen only in response to cellular injury, but not during normal developmental apoptosis. In particular, inactivation of DIAP1 by Reaper, Hid, and Grim is restricted not only to injury-provoked apoptosis, but also underlies most developmental cell deaths (White et al., 1994; Lohmann et al., 2002; Yu et al., 2002). One possible explanation is that activation of the JNK pathway is key to mitogenic signaling of apoptotic cells. Consistent with this idea, the JNK pathway is activated in response to tissue stress and injury, but not during developmental apoptosis (Adachi-Yamada et al., 1999; Moreno et al., 2002; Martin-Blanco et al., 1998; H.D.R. and H.S., unpublished data). Furthermore, in this study we show that JNK signaling can induce the expression of *wg*/*dpp* and nonautonomous cell proliferation. Therefore, it is possible that robust JNK activation and compensatory proliferation require the combined input of stress and apoptotic signals (Figure 8).

wg Signaling Is Required for Cell Proliferation

The role of *wg* signaling in cell proliferation has remained controversial. *wg* is required for disc growth and is sufficient to promote proliferation in proximal discs (Figure 6; Neumann and Cohen, 1996). However, mosaic analyses of *wg* pathway genes in imaginal discs also indicated that *wg* signaling constrains cell proliferation in distal parts of imaginal discs (Johnston and Sanders, 2003). These previous studies relied on clonal analyses, which are typically performed several days after manipulation. Such a long time course allows for a multitude of secondary effects. We have attempted to improve upon such pitfalls by using a conditional gene activation system to examine the mitogenic effect of *wg* signaling over a short time course (12 hr). Our results indicate that *wg* signaling is required for cell proliferation and hence may contribute to the regulation of normal disc growth. In addition, we found that compensatory proliferation cannot bypass the requirement for *wg* signaling. However, our results do not exclude the possibility that additional mitogens are required.

Implications in Cancer and Growth Control

Besides its contribution to compensatory proliferation in *Drosophila* imaginal discs, mitogenic signaling in response to stress-induced apoptosis may be a more general and an evolutionary conserved phenomenon. For example, hallmarks of cancer include apoptotic stress, such as genetic instability, as well as defective apoptosis (Hanahan and Weinberg, 2000). This combination may generate undead cells in tumor tissues that promote further tumor growth. Also, mice with disrupted apoptosis genes exhibit brains that resemble hyperplasia (e.g., in caspase-9 and Apaf-1 mutants). Although

this has been largely attributed to the failure to eliminate excessive cells through apoptosis, a recent study has reported extraproliferation as a secondary consequence of defective apoptosis (Li et al., 2003). Based on the behavior of undead cells in *Drosophila* imaginal discs, one might expect mutations that block or delay apoptosis to cause secondary proliferation and hyperplasia. It remains to be tested if such a mechanism contributes to hyperplasia in mouse models and human malignancies.

Experimental Procedures

Fly Strains and Crosses

All flies were raised at room temperature (21°C) unless stated otherwise. FRT/FLP-mediated mitotic recombination (Xu and Rubin, 1993) and the Gal4/UAS system (Brand and Perrimon, 1993) were used to generate undead cells. *diap1* alleles *diap1*^{th5}, *diap1*$^{33\text{-}1s}$, and *diap1*$^{22\text{-}8s}$ were recombined with *75CP[w+],FRT80* chromosome to generate *diap1, FRT80* chromosomes. *th5* is a null allele, whereas *22-8s* and *33-1s* are partial loss-of-function alleles with impaired RING domains (Goyal et al., 2000; Wilson et al., 2002). For cell lethality assay of *diap1*$^{22\text{-}8s}$*, yw, hs-flp; hs-GFP, FRT80* flies were crossed to *diap1*$^{22\text{-}8s}$*, FRT80/TM6B* flies. In Figure 1, mitotic recombination was induced by 1 hr heat shock at 37°C. Here, the *diap1*$^{22\text{-}8s/22\text{-}8s}$ population was marked by the absence of GFP. GFP was visualized by 1 hr heat shock at 37°C prior to dissection, which alone did not cause cell death as assayed by anti-active caspase-3 labeling (data not shown). The *75CP[w+],FRT80* chromosome was used to generate control mosaic clones. In order to generate *diap1*$^{-/-}$ undead clones within the P compartment, *en-Gal4, dpp-lacZ ; ubi-GFP, FRT80* flies were crossed to *uas-p35, uas-flp; diap1, FRT80/TM6B* flies. As a control, *uas-flp; diap1, FRT80/TM6B* flies were crossed to *en-Gal4, dpp-lacZ; ubi-GFP, FRT80* flies. For similar clones in the eye, *ey-Gal4* driver was used instead of *en-Gal4*.

To generate *hid*- or *rpr*-expressing undead cells, *uas-hid; uas-p35* or *uas-rpr; uas-p35* flies were crossed to the relevant Gal4 drivers. Flip out clones expressing transgenes were generated as described previously (Zecca and Struhl, 2002). In specific, the UAS transgenic lines were crossed to *yw, hs-flp* ^{122}*; tubulin*α*1*>*y+, GFP*>*Gal4* line, heat shocked for 30 min at 37°C, and fixed after defined time points for immunohistochemistry. To inhibit the JNK pathway or Dronc, *uas-hid; uas-p35; uas-puc* or *uas-hid; uas-p35; uas-dronc*^{DN} were used. *uas-dronc*^{DN} is as described (Meier et al., 2000). For *puc* genetic interaction assay, en-*Gal4; puc*^{E69}*/TM6B* flies were crossed to the relevant *uas* lines.

Temporal activation of *hep*^{CA20} and *TCF*^{DN24} were done using the Gal4/Gal80^{ts} system (McGuire et al., 2003). *en-Gal4* is completely inhibited by *tub-Gal80*^{ts} at 18°C. In specific, we crossed *wg-lacZ, en-Gal4; tub-Gal80*^{ts} or *dpp-lacZ, en-Gal4; tub-Gal80*^{ts} flies to the relevant UAS lines. Gal4 was activated at 29°C and the animals were dissected at specific time points as mentioned in the text. To activate *wg* signaling, *uas-*Δ*arm* (Zecca et al., 1996) was crossed to *yw, hs-flp*^{122}*; tubulin*α*1*>*y+, GFP*>*Gal4*.

Immunohistochemistry and BrdU Labeling

Rabbit or guinea pig anti-Hid antibody was raised against full-length Hid fused to GST and was subsequently affinity purified. Guinea pig anti-Dronc antibody was raised against a near full-length Dronc$^{C\rightarrow A}$ (starts at aa 6 and stops 5 aa before the stop codon) fused to His-tag. The catalytic site mutation of this construct is as described (Meier et al., 2000). Commercial antibodies used in this work are monoclonal anti-WG antibody (4D4) (U. of Iowa, DSHB), polyclonal mouse anti-β-gal (Sigma), mouse anti-BrdU antibody (BD PharMingen), and rabbit anti-active caspase-3 antibody (Cell Signaling Technology). Immunohistochemistry was done on late third instar larval imaginal discs based on standard protocols. BrdU was labeled for 30 min and standard protocols were followed thereafter (de Nooij et al., 1996; Schubiger and Palka, 1987).

Size Measurement

To compare the size of wing imaginal discs, the animals were reared in similar growth conditions, and the wing imaginal discs of wandering stage third larvae were analyzed. The images of wing discs were taken with a 10× objective lens after fixation. Size was quantified through the "histogram" function in Adobe Photoshop 6.0. The measurement was repeated through independent fly crosses and their statistical significance was evaluated through a two-tailed, unpaired Student's t test.

To measure the size of wing discs in Figure 6I, undead clones were induced by heat shocking larvae for 30 min, and the wandering stage larval imaginal discs were analyzed 48 hr afterwards. As controls, sibling larvae that lacked *hs-flp* were reared in the same vials and analyzed under identical conditions.

Acknowledgments

We thank the Steller lab members and A. Ciechanover for discussion and criticism; G. Halder, R. Mann, B. Mollereau, and S. Sachse for technical advice; R. Cisse for technical aid; S. Shaham for critically reading the manuscript; T. Adachi-Yamada, K. Basler, G. Struhl, R. Mann, and the Bloomington stock center for fly stocks; and G. Morata for communicating unpublished results. H.D.R. was a fellow of the Leukemia-Lymphoma Society. H.S. is an investigator of the Howard Hughes Medical Institute. This work was supported by NIH grant RO1 GM60124.

Received: July 12, 2004
Revised: August 31, 2004
Accepted: August 31, 2004
Published online: September 16, 2004

References

Adachi-Yamada, T., Fujimura-Kamada, K., Nishida, Y., and Matsumoto, K. (1999). Distortion of proximodistal information causes JNK-dependent apoptosis in *Drosophila* wing. Nature *400*, 166–169.

Brand, A.H., and Perrimon, N. (1993). Targeted gene expression as a means of altering cell fates and generating dominant phenotypes. Development *118*, 401–415.

Brodsky, M.H., Nordstrom, W., Tsang, G., Kwan, E., Rubin, G.M., and Abrams, J.M. (2000). *Drosophila* p53 binds a damage response element at the reaper locus. Cell *101*, 103–113.

Bryant, P.J. (1971). Regeneration and duplication following operations in situ on the imaginal discs of *Drosophila melanogaster*. Dev. Biol. *26*, 637–651.

Burke, R., and Basler, K. (1996). Dpp receptors are autonomously required for cell proliferation in the entire developing *Drosophila* wing. Development *122*, 2261–2269.

Chen, P., Nordstrom, W., Gish, B., and Abrams, J.M. (1996). *grim*, a novel cell death gene in *Drosophila*. Genes Dev. *10*, 1773–1782.

Clem, R.J., Fechneimer, M., and Miller, L.K. (1991). Prevention of apoptosis by a baculovirus gene during infection of insect cells. Science *254*, 1388–1390.

Daniel, N., and Korsmeyer, S. (2004). Cell death: critical control points. Cell *116*, 205–219.

De Nooij, J.C., Letendre, M.A., and Hariharan, I.K. (1996). A cyclin-dependent kinase inhibitor, Decapo, is necessary for timely exit from the cell cycle during *Drosophila* embryogenesis. Cell *87*, 1237–1247.

Fraser, A.G., McCarthy, N.J., and Evan, G.I. (1997). drICE is an essential caspase required for apoptotic activity in *Drosophila* cells. EMBO J. *16*, 6192–6199.

Garcia-Bellido, A., Ripoll, P., and Morata, G. (1973). Developmental compartmentalization of the wing disc of *Drosophila*. Nat. New Biol. *245*, 251–253.

Gibson, M.C., and Schubiger, G. (1999). Hedgehog is required for activation of engrailed during regeneration of fragmented *Drosophila* imaginal discs. Development *126*, 1591–1599.

Goyal, L., McCall, K., Agapite, J., Hartwieg, E., and Steller, H. (2000). Induction of apoptosis by Drosophila reaper, hid and grim through inhibition of IAP function. EMBO J. *19*, 589–597.

Grether, M.E., Abrams, J.M., Agapite, J., White, K., and Steller, H. (1995). The head involution defective gene of *Drosophila melanogaster* functions in programmed cell death. Genes Dev. *9*, 1694–1708.

Hanahan, D., and Weinberg, R.A. (2000). The hallmarks of cancer. Cell *100*, 57–70.

Haynie, J.L., and Bryant, P.J. (1977). The effects of X-rays on the proliferation dynamics of cells in the imaginal wing disc of *Drosophila melanogaster*. Rouxs Arch. Dev. Biol. *183*, 85–100.

Hengartner, M.O. (2000). The biochemistry of apoptosis. Nature *407*, 770–776.

Huh, J., Guo, M., and Hay, B.A. (2004). Compensatory proliferation induced by cell death in the *Drosophila* wing disc requires activity of the apical cell death caspase in a nonapoptotic role. Curr. Biol. *14*, 1262–1266.

Jacobson, M.D., Weil, M., and Raff, M.C. (1997). Programmed cell death in animal development. Cell *88*, 347–354.

Johnston, L.A., and Sanders, A.L. (2003). Wingless promotes cell survival but constrains growth during *Drosophila* wing development. Nat. Cell Biol. *5*, 827–833.

Kerr, J.F.R., Wyllie, A.H., and Currie, A.R. (1972). Apoptosis: a basic biological phenomenon with wide-ranging implications in tissue kinetics. Br. J. Cancer *26*, 239–257.

Kuranaga, E., Kanuka, H., Igaki, T., Sawamoto, K., Ichijo, H., Okano, H., and Miura, M. (2002). Reaper-mediated inhibition of DIAP1-induced DTRAF1 degradation results in activation of JNK in *Drosophila*. Nat. Cell Biol. *4*, 705–710.

Li, X., Yang, Y., and Ashwell, J.D. (2002). TNF-RII and c-IAP1 mediate ubiquitination and degradation of TRAF2. Nature *416*, 345–347.

Li, M.O., Sarkisian, M.R., Mehal, W.Z., Rakic, P., and Flavell, R.A. (2003). Phosphatidylserine receptor is required for clearance of apoptotic cells. Science *302*, 1560–1563.

Lisi, S., Mazzon, I., and White, K. (2000). Diverse domains of THREAD/DIAP1 are required to inhibit apoptosis induced by REAPER and HID in Drosophila. Genetics *154*, 669–678.

Lohmann, I., McGinnis, N., Bodmer, M., and McGinnis, W. (2002). The *Drosophila* Hox gene deformed sculpts head morphology via direct regulation of the apoptosis activator reaper. Cell *110*, 457–466.

Martin-Blanco, E., Gampel, A., Ring, J., Virdee, K., Kirov, N., Tolkovsky, A.M., and Martinez-Arias, A. (1998). puckered encodes a phosphatase that mediates a feedback loop regulating JNK activity during dorsal closure in *Drosophila*. Genes Dev. *12*, 557–570.

Martin-Castellanos, C., and Edgar, B.A. (2002). A characterization of the effects of Dpp signaling on cell growth and proliferation in the *Drosophila* wing. Development *129*, 1003–1013.

McGuire, S.E., Le, P.T., Osborn, A.J., Matsumoto, K., and Davis, R.L. (2003). Spatiotemporal rescue of memory dysfunction in *Drosophila*. Science *302*, 1765–1768.

Meier, P., Silke, J., Leevers, S.J., and Evan, G. (2000). The *Drosophila* caspase DRONC is regulated by DIAP1. EMBO J. *19*, 598–611.

Milan, M., Baonza, A., and Garcia-Bellido, A. (1997). Developmental parameters of cell death in the wing disc of *Drosophila*. Proc. Natl. Acad. Sci. USA *94*, 5691–5696.

Moreno, E., Basler, K., and Morata, G. (2002). Cells compete for decapentaplegic survival factor to prevent apoptosis in *Drosophila* wing development. Nature *416*, 755–759.

Neufeld, T.P., de la Cruz, A.F., Johnston, L.A., and Edgar, B.A. (1998). Coordination of growth and cell division in the *Drosophila* wing. Cell *93*, 1183–1193.

Neumann, C.J., and Cohen, S.M. (1996). Distinct mitogenic and cell fate specification functions of wingless in different regions of the wing. Development *122*, 1781–1789.

Ryoo, H.D., Bergmann, A., Gonen, H., Ciechanover, A., and Steller, H. (2002). Regulation of *Drosophila* IAP1 degradation and apoptosis by reaper and ubcD1. Nat. Cell Biol. *4*, 432–438.

Salvesen, G.S., and Abrams, J.M. (2004). Caspase activation—stepping on the gas or releasing the brakes? Lessons from humans and flies. Oncogene *23*, 2774–2784.

Schubiger, M., and Palka, J. (1987). Changing spatial patterns of DNA replication in the developing wing of *Drosophila*. Dev. Biol. *123*, 145–153.

Song, Z., McCall, K., and Steller, H. (1997). DCP-1, a *Drosophila* cell death protease essential for development. Science *275*, 536–540.

van de Weterling, M., Cavallo, R., Dooijes, D., van Beest, M., van Es, J., Loureiro, J., Ypma, A., Hursh, D., Jones, T., Bejsovec, A., et al. (1997). Armadillo coactivates transcription driven by the product of the *Drosophila* segment polarity gene dTCF. Cell *88*, 789–799.

Wang, S.L., Hawkins, C.J., Yoo, S.J., Muller, H.A., and Hay, B.A. (1999). The *Drosophila* caspase inhibitor DIAP1 is essential for cell survival and is negatively regulated by HID. Cell *98*, 453–463.

White, K., Grether, M.E., Abrams, J.M., Young, L., Farrell, K., and Steller, H. (1994). Genetic control of programmed cell death in *Drosophila*. Science *264*, 677–683.

Wilson, R., Goyal, L., Ditzel, M., Zachariou, A., Baker, D.A., Agapite, J., Steller, H., and Meier, P. (2002). The DIAP1 RING finger mediates ubiquitination of Dronc and is indispensable for regulating apoptosis. Nat. Cell Biol. *4*, 445–450.

Xu, T., and Rubin, G.M. (1993). Analysis of genetic mosaics in developing and adult *Drosophila* tissues. Development *117*, 1223–1237.

Yoo, S.J., Huh, J.R., Muro, I., Yu, H., Wang, L., Wang, S.L., Feldman, R.M., Clem, R.J., Muller, H.A., and Hay, B.A. (2002). Hid, Rpr and Grim negatively regulate DIAP1 levels through distinct mechanisms. Nat. Cell Biol. *4*, 416–424.

Yu, S.Y., Yoo, S.J., Yang, L., Zapata, C., Srinivasan, A., Hay, B.A., and Baker, N.E. (2002). A pathway of signals regulating effector and initiator caspases in the developing *Drosophila* eye. Development *129*, 3269–3278.

Yuan, J., Shaham, S., Ledoux, S., Ellis, H.M., and Horvitz, H.R. (1993). The *C. elegans* cell death gene ced-3 encodes a protein similar to mammalian interleukin-1 beta converting enzyme. Cell *75*, 641–652.

Zecca, M., and Struhl, G. (2002). Subdivision of the *Drosophila* wing imaginal disc by EGFR-mediated signaling. Development *129*, 1357–1368.

Zecca, M., Basler, K., and Struhl, G. (1996). Direct and long range action of a wingless morphogen gradient. Cell *87*, 833–884.

Zhou, L., and Steller, H. (2003). Distinct pathways mediate UV-induced apoptosis in *Drosophila* embryos. Dev. Cell *4*, 599–605.

Note Added in Proof

Gines Morata and colleagues independently report that cells undergoing apoptosis in response to X-ray or heat shock express *wg* and *dpp* (Perez-Garijo, A., Martin, F.A., and Morata, G. (2004). Caspase inhibition during apoptosis causes abnormal signaling and developmental aberrations in *Drosophila*. Development, in press.).